EINDHOVEN UNIVERSITY OF TECHNOLOGY

The finite volume-complete flux scheme for one-dimensional advection-diffusion-reaction equations

Citation for published version (APA):
Thije Boonkkamp, ten, J. H. M., & Anthonissen, M. J. H. (2008). *The finite volume-complete flux scheme for one-dimensional advection-diffusion-reaction equations*. (CASA-report; Vol. 0828). Technische Universiteit Eindhoven.

Document status and date:
Published: 01/01/2008

Document Version:
Publisher's PDF, also known as Version of Record (includes final page, issue and volume numbers)

Please check the document version of this publication:

• A submitted manuscript is the version of the article upon submission and before peer-review. There can be important differences between the submitted version and the official published version of record. People interested in the research are advised to contact the author for the final version of the publication, or visit the DOI to the publisher's website.
• The final author version and the galley proof are versions of the publication after peer review.
• The final published version features the final layout of the paper including the volume, issue and page numbers.

Link to publication

General rights
Copyright and moral rights for the publications made accessible in the public portal are retained by the authors and/or other copyright owners and it is a condition of accessing publications that users recognise and abide by the legal requirements associated with these rights.

• Users may download and print one copy of any publication from the public portal for the purpose of private study or research.
• You may not further distribute the material or use it for any profit-making activity or commercial gain
• You may freely distribute the URL identifying the publication in the public portal.

If the publication is distributed under the terms of Article 25fa of the Dutch Copyright Act, indicated by the "Taverne" license above, please follow below link for the End User Agreement:

www.tue.nl/taverne

Take down policy
If you believe that this document breaches copyright please contact us at:

openaccess@tue.nl

providing details and we will investigate your claim.

Download date: 04. Oct. 2023

The finite volume-complete flux scheme for one-dimensional advection-diffusion-reaction equations

J.H.M. ten Thije Boonkkamp and M.J.H. Anthonissen
Department of Mathematics and Computer Science, Eindhoven University of Technology
P.O. Box 513, 5600 MB Eindhoven, The Netherlands

Abstract

We present a new integral representation for the flux of the advection-diffusion-reaction equation, which is based on the solution of a local boundary value problem for the *entire* equation, including the source term. The flux therefore consists of two parts, corresponding to the homogeneous and particular solution of the boundary value problem. Applying suitable quadrature rules to the integral representation gives the complete flux scheme, which is second order accurate, uniformly in the local Peclet numbers. The flux approximation is combined with a finite volume method, and the resulting finite volume-complete flux scheme is validated for several test problems.

Keywords. Advection-diffusion-reaction equation, flux, finite volume method, integral representation of the flux, numerical flux, compressible Navier-Stokes equations.
AMS subject classifications. 34B05, 34B99, 65D30, 65L10, 65L99, 76N15.

1 Introduction

Conservation laws are ubiquitous in continuum physics, they occur in disciplines like fluid mechanics, combustion theory, plasma physics, semiconductor physics etc. These conservation laws are often of advection-diffusion-reaction type, describing the interplay between different processes such as advection or drift, diffusion or conduction and (chemical) reaction or recombination/generation. Examples are the conservation equations for reacting flow [14, 24] or the drift-diffusion equations for semiconductor devices [8, 10].

Their numerical solution requires at least an adequate (space) discretisation. There are many (classes of) methods available, such as finite element, finite difference, finite volume or spectral methods. We restrict ourselves to finite volume methods; for a detailed account see e.g. [5, 11, 23]. Finite volume methods are based on the integral formulation, i.e., the conservation law is integrated over a disjunct set of control volumes covering the domain. The resulting discrete conservation law involves fluxes at the interfaces of the control volumes, which need to be approximated.

Our objective in this paper is to present new expressions for the flux, which will subsequently be used to derive numerical flux approximations. We restrict ourselves to steady, one-dimensional conservation equations. Moreover, we require that the numerical flux has the following properties. First, it should be unconditionally second order accurate, in particular, the flux approximation should remain second order accurate for highly dominant advection. This excludes the hybrid scheme of Spalding [18], which reduces to the standard upwind scheme when diffusion is absent. Second, the numerical flux should not produce spurious oscillations for dominant advection, as the standard central difference scheme does,

and third, the flux may only depend on neighbouring values of the unknown, resulting in a three-point scheme. The latter requirement rules out high resolution schemes based on flux/slope limiters [9, 23] or (W)ENO reconstruction [17].

Our scheme is inspired by two papers by Thiart [19, 20]. In these papers a finite volume method is combined with an exponential scheme for the flux. More specifically, the fluxes at the cell interfaces are computed from a local boundary value problem, assuming piecewise constant coefficients. The source term is included in the computation of the fluxes. Similar schemes have been published the in last few decades. Without trying to be complete, we just mention a few. Allen and Southwell [1] and Il'in [7] introduced an exponentially fitted scheme, which is a hybrid central difference-upwind scheme such that the difference scheme locally has the same (exponential) solutions as the corresponding differential equation. An improvement of this scheme is proposed by El-Mistikawy and Werle [4]. These exponentially fitted schemes are a special case of the so-called locally exact schemes. The basic idea is to represent the solution in two adjacent intervals in terms of an approximate Green's function; see [11] and references therein. Exponentially fitted schemes are nowadays widely used to simulate advection-diffusion-reaction problems from continuum physics, especially to compute numerical solutions of the drift-diffusion model for semiconductor devices. For this application these schemes are known as the Scharfetter-Gummel scheme; see e.g. [3, 16]. An extension of the Scharfetter-Gummel scheme to describe avalanche generation is presented in [22]. In this extended scheme, the avalanche generation/recombination source terms are included in the numerical fluxes.

Our scheme is an extension of the schemes by Thiart. We derive an integral representation for the flux from the solution of a local boundary value problem for the *entire* equation, including the source term, but we do not restrict ourselves to (locally) constant coefficients. As a consequence, the flux has a homogeneous and an inhomogeneous component, corresponding to the homogeneous and the particular solution of the boundary value problem, respectively. Suitable quadrature rules are applied to derive the numerical flux. The inclusion of the inhomogeneous flux will be of importance when advection dominates diffusion.

We have organized our paper as follows. The finite volume method is briefly summarized in Section 2. In Section 3 we derive an integral representation for the flux, in terms of a Green's function, which will be used in Section 4 to derive the numerical flux approximation, referred to as the complete flux scheme. The combined complete flux-finite volume scheme is presented in Section 5. To test the scheme, we apply it in Section 6 to several model problems. Finally, we end with a summary and conclusions in Section 7.

2 Finite volume discretisation

In this section we outline the finite volume method (FVM) for a generic conservation law of advection-diffusion-reaction type. So, consider the following conservation law defined on the interval (a, b),

$$\big(m\varphi - \varepsilon\varphi'\big)' = s, \tag{2.1}$$

where m is the mass flux, $\varepsilon \geq \varepsilon_{\min} > 0$ a diffusion/conduction coefficient and s a (chemical) source term. The unknown φ can be, e.g., the temperature or the concentration of a species in a reacting flow. The parameters ε and s are usually (complicated) functions of the unknown φ, however, for the sake of discretisation we will consider these as given functions of the spatial coordinate x. The mass flux m generally has to be computed from the flow equations corresponding to (2.1), but in this paper it is assumed to be a given function of x as well. Equations of this type arise, e.g., in combustion theory [14].

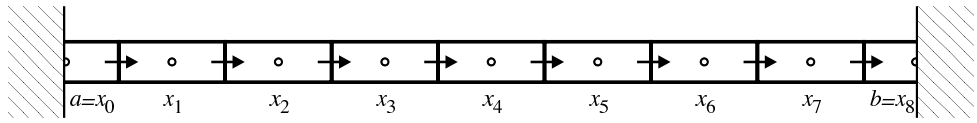

Figure 1: The finite volume grid on the interval $[a, b]$.

Associated with equation (2.1) we introduce the flux f, defined by

$$f := m\varphi - \varepsilon\varphi'. \tag{2.2}$$

Equation (2.1) then reduces to $f' = s$. Integrating this equation over an arbitrary interval $[\alpha, \beta] \subset [a, b]$ we obtain the integral form of the conservation law, i.e.,

$$f(\beta) - f(\alpha) = \int_\alpha^\beta s(x)\,\mathrm{d}x. \tag{2.3}$$

This equation is in fact the basic conservation law, which reduces to (2.1) provided φ is smooth enough.

In the FVM we cover $[a, b]$ with a finite number of disjunct intervals (control volumes) I_j of size Δx as shown in Figure 1. Moreover, we have to define a spatial grid $\{x_j\}$ where the variable φ has to be approximated. In this paper we choose the cell-centred approach [23], i.e., we choose the grid point x_j in the centre of the jth interval I_j. Consequently we have $I_j := [x_{j-1/2}, x_{j+1/2}]$ with $x_{j+1/2} := \frac{1}{2}(x_j + x_{j+1})$. Imposing the integral form (2.3) on each of the intervals I_j, we obtain the discrete conservation law

$$F_{j+1/2} - F_{j-1/2} = Q_j(s), \tag{2.4}$$

where $F_{j+1/2}$ is the numerical flux approximating f at $x = x_{j+1/2}$ and where $Q_j(s)$ is a quadrature rule for the integral of s over I_j. In this paper, we will adopt the midpoint rule, resulting in

$$F_{j+1/2} - F_{j-1/2} = s_j\,\Delta x, \tag{2.5}$$

with $s_j := s(x_j)$. The FVM has to be completed with expressions for the numerical flux. We require that the numerical flux $F_{j+1/2}$ linearly depends on φ and s in the neighbouring grid points x_j and x_{j+1}, i.e., we are looking for an expression of the form

$$F_{j+1/2} = \alpha_{j+1/2}\,\varphi_j - \beta_{j+1/2}\,\varphi_{j+1} + \gamma_{j+1/2}\,s_j + \delta_{j+1/2}\,s_{j+1}, \tag{2.6}$$

where the coefficients $\alpha_{j+1/2}$ etc. only depend on m and ε. Substitution of this expression in the discrete conservation law (2.5) leads to a tridiagonal linear system for the vector of unknowns $\boldsymbol{\varphi} = (\varphi_j)$. The procedure to compute $F_{j+1/2}$ is detailed in the next two sections.

3 Integral representation for the flux

Our objective in this section is to derive an integral representation for the flux. The derivation is a modification of the theory in [6].

We adopt the following notation: variables defined in the grid points x_j and x_{j+1} are indicated with the subscripts C (centre) and E (east), respectively, and variables at the cell edge $x_{j+1/2}$ by the subscript

e (east). The derivation of the expression for the flux f_{e} at the eastern cell edge x_{e} located between the grid points x_{C} and x_{E} is based on the following model boundary value problem (BVP) for the unknown φ:

$$\big(m\varphi - \varepsilon\varphi'\big)' = s, \quad x_{\mathrm{C}} < x < x_{\mathrm{E}}, \tag{3.1a}$$

$$\varphi(x_{\mathrm{C}}) = \varphi_{\mathrm{C}}, \quad \varphi(x_{\mathrm{E}}) = \varphi_{\mathrm{E}}. \tag{3.1b}$$

We like to emphasize that f_{e} corresponds to the solution of the *inhomogeneous* BVP (3.1), implying that f_{e} not only depends on m and ε but on s as well.

In the following, we need the variables λ, P, Λ and S, defined by

$$\lambda := \frac{m}{\varepsilon}, \quad P := \lambda\Delta x, \quad \Lambda(x) := \int_{x_{\mathrm{e}}}^{x} \lambda(\xi)\,\mathrm{d}\xi, \quad S(x) := \int_{x_{\mathrm{e}}}^{x} s(\xi)\,\mathrm{d}\xi, \tag{3.2}$$

with $\Delta x := x_{\mathrm{E}} - x_{\mathrm{C}}$. We refer to the variables P and Λ as the (numerical) Peclet function and Peclet integral, respectively, generalizing the well-known (numerical/grid) Peclet number [23]. Integrating equation (3.1a) we get the following integral balance

$$f(x) - f_{\mathrm{e}} = S(x). \tag{3.3}$$

Using the definition of Λ in (3.2), it is clear that expression (2.2) for the flux can be rewritten as

$$f = -\varepsilon\big(\varphi\,\mathrm{e}^{-\Lambda}\big)'\mathrm{e}^{\Lambda}. \tag{3.4}$$

Substituting (3.4) in (3.3) and once more integrating we obtain the following expression for the flux f_{e}:

$$f_{\mathrm{e}} = f_{\mathrm{e}}^{(\mathrm{h})} + f_{\mathrm{e}}^{(\mathrm{i})}, \tag{3.5a}$$

$$f_{\mathrm{e}}^{(\mathrm{h})} = -\big(\mathrm{e}^{-\Lambda_{\mathrm{E}}}\varphi_{\mathrm{E}} - \mathrm{e}^{-\Lambda_{\mathrm{C}}}\varphi_{\mathrm{C}}\big) \Big/ \int_{x_{\mathrm{C}}}^{x_{\mathrm{E}}} \varepsilon^{-1}\mathrm{e}^{-\Lambda}\,\mathrm{d}x, \tag{3.5b}$$

$$f_{\mathrm{e}}^{(\mathrm{i})} = -\int_{x_{\mathrm{C}}}^{x_{\mathrm{E}}} \varepsilon^{-1}\mathrm{e}^{-\Lambda} S\,\mathrm{d}x \Big/ \int_{x_{\mathrm{C}}}^{x_{\mathrm{E}}} \varepsilon^{-1}\mathrm{e}^{-\Lambda}\,\mathrm{d}x, \tag{3.5c}$$

where $f_{\mathrm{e}}^{(\mathrm{h})}$ and $f_{\mathrm{e}}^{(\mathrm{i})}$ are the homogeneous and inhomogeneous part, corresponding to the homogeneous and particular solution of (3.1), respectively.

Assume first that m, ε and s are constant on the interval $[x_{\mathrm{C}}, x_{\mathrm{E}}]$. In this case we can determine all integrals in (3.2). The Peclet function reduces to the Peclet number, i.e., $P = m\Delta x/\varepsilon$. Furthermore, $\Lambda(x) = \lambda(x - x_{\mathrm{e}})$ and $S(x) = s(x - x_{\mathrm{e}})$. Substituting these expressions in (3.5b) and (3.5c) and evaluating all integrals involved, we find

$$f_{\mathrm{e}}^{(\mathrm{h})} = -\frac{\varepsilon}{\Delta x}\big(B(P)\varphi_{\mathrm{E}} - B(-P)\varphi_{\mathrm{C}}\big), \tag{3.6a}$$

$$f_{\mathrm{e}}^{(\mathrm{i})} = \big(\tfrac{1}{2} - W(P)\big)s\,\Delta x. \tag{3.6b}$$

Here we have used the Bernoulli function B and the function W, defined by

$$B(z) := \frac{z}{\mathrm{e}^{z} - 1}, \quad W(z) := \frac{\mathrm{e}^{z} - 1 - z}{z\big(\mathrm{e}^{z} - 1\big)}; \tag{3.7}$$

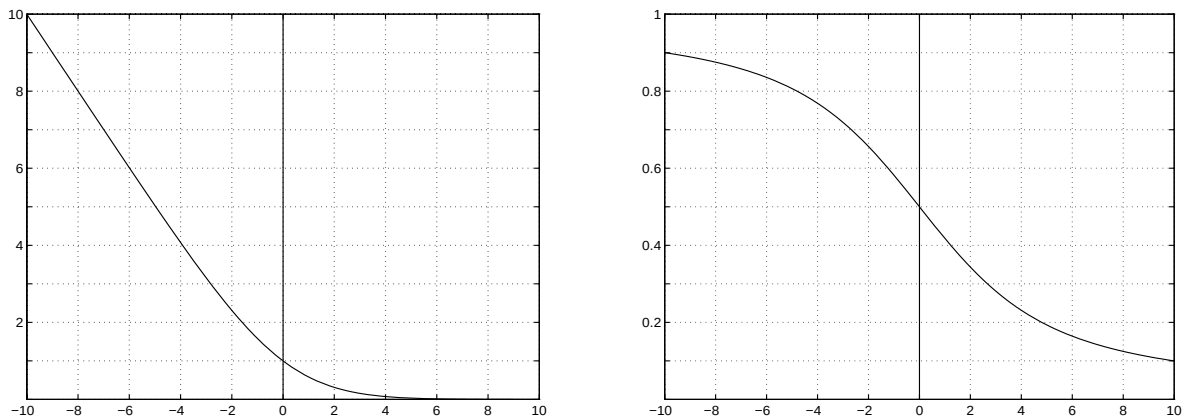

Figure 2: The Bernoulli function $B(z)$ (left) and the function $W(z)$ (right).

see Figure 2. Note that W satisfies $0 \leq W(z) \leq 1$ and $W(-z)+W(z) = 1$. Clearly, the inhomogeneous flux is of importance when $|P| \gg 1$, i.e., for advection dominated flow. For the constant coefficient homogeneous flux we introduce the function

$$f_{\mathrm{e}}^{(\mathrm{h})} = \mathcal{F}^{\mathrm{h}}\big(\varepsilon/\Delta x, P; \varphi_{\mathrm{C}}, \varphi_{\mathrm{E}}\big) = \alpha_{\mathrm{e}}\big(\varepsilon/\Delta x, P\big)\varphi_{\mathrm{C}} - \beta_{\mathrm{e}}\big(\varepsilon/\Delta x, P\big)\varphi_{\mathrm{E}}, \tag{3.8}$$

to denote the dependence of $f_{\mathrm{e}}^{(\mathrm{h})}$ on the parameters $\varepsilon/\Delta x$ and P and on the function values φ_{C} and φ_{E}. The constant coefficient homogeneous flux is often used as approximation of the flux (2.2); see e.g. [13].

We will now generalize the constant coefficient fluxes (3.6a) and (3.6b) for the case of nonconstant m, ε and s. Let $\langle a, b\rangle$ denote the usual inner product of two functions $a = a(x)$ and $b = b(x)$ defined on $(x_{\mathrm{C}}, x_{\mathrm{E}})$, i.e.,

$$\langle a, b\rangle := \int_{x_{\mathrm{C}}}^{x_{\mathrm{E}}} a(x)b(x)\,\mathrm{d}x. \tag{3.9}$$

For arbitrary m, ε and s the homogeneous flux can be written as a modification of the constant coefficient flux and the inhomogeneous flux as a weighted average of the integrated source term S as follows:

$$f_{\mathrm{e}}^{(\mathrm{h})} = \mathcal{F}^{\mathrm{h}}\Big(\frac{\langle\lambda, \mathrm{e}^{-\Lambda}\rangle/\langle\lambda, 1\rangle}{\langle\varepsilon^{-1}, \mathrm{e}^{-\Lambda}\rangle}, \langle\lambda, 1\rangle; \varphi_{\mathrm{C}}, \varphi_{\mathrm{E}}\Big), \tag{3.10a}$$

$$f_{\mathrm{e}}^{(\mathrm{i})} = -\frac{\langle\varepsilon^{-1}S, \mathrm{e}^{-\Lambda}\rangle}{\langle\varepsilon^{-1}, \mathrm{e}^{-\Lambda}\rangle}. \tag{3.10b}$$

Our numerical approximation of the homogeneous flux will be based on (3.10a). For the inhomogeneous flux we derive an alternative expression. Substituting the expression for S in (3.5c) and changing the order of integration we find the following representation for the inhomogeneous flux

$$f_{\mathrm{e}}^{(\mathrm{i})} = \Delta x \int_0^1 G(\sigma)s(x(\sigma))\,\mathrm{d}\sigma, \quad \sigma(x) := \frac{x - x_{\mathrm{C}}}{\Delta x}, \tag{3.11}$$

where $\sigma = \sigma(x)$ is the normalised coordinate on $[x_{\mathrm{C}}, x_{\mathrm{E}}]$ and $x = x(\sigma)$ its inverse, and where $G(\sigma)$ is

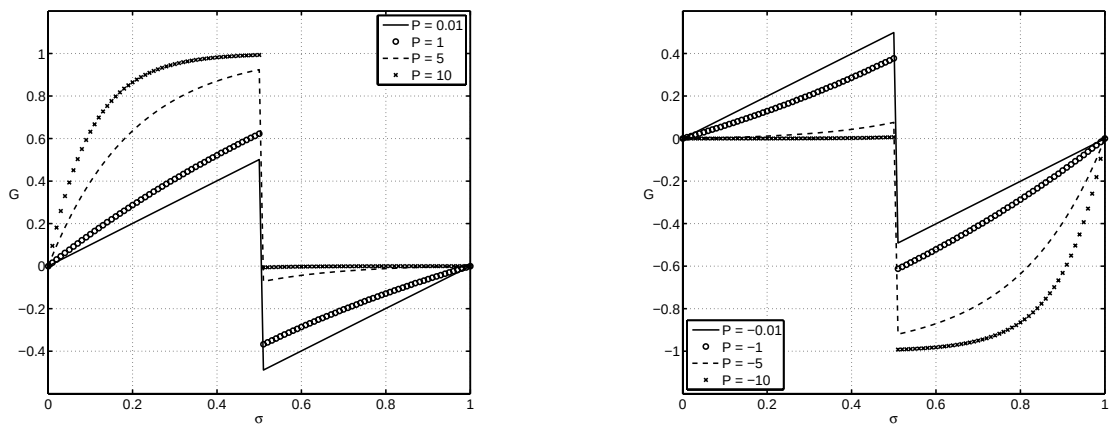

Figure 3: Green's function for the flux for $P > 0$ (left) and $P < 0$ (right).

the Green's function for the flux, given by

$$G(\sigma) = \begin{cases} \Delta x \displaystyle\int_0^\sigma \varepsilon^{-1}(x(\eta))\, \mathrm{e}^{-\Lambda(x(\eta))}\, \mathrm{d}\eta / \langle \varepsilon^{-1}, \mathrm{e}^{-\Lambda} \rangle & \text{for} \quad 0 \le \sigma \le \frac{1}{2}, \\ -\Delta x \displaystyle\int_\sigma^1 \varepsilon^{-1}(x(\eta))\, \mathrm{e}^{-\Lambda(x(\eta))}\, \mathrm{d}\eta / \langle \varepsilon^{-1}, \mathrm{e}^{-\Lambda} \rangle & \text{for} \quad \frac{1}{2} < \sigma \le 1, \end{cases} \tag{3.12}$$

with $x(\eta) := x_\mathrm{C} + \eta \Delta x$. Note that G relates the *flux* to the source term and is different from the usual Green's function, which relates the *solution* to the source term [11]. For the special case of constant m and ε the Green's function reduces to

$$G(\sigma; P) = \begin{cases} \dfrac{1 - \mathrm{e}^{-P\sigma}}{1 - \mathrm{e}^{-P}} & \text{for} \quad 0 \le \sigma \le \frac{1}{2}, \\ -\dfrac{1 - \mathrm{e}^{P(1-\sigma)}}{1 - \mathrm{e}^{P}} & \text{for} \quad \frac{1}{2} < \sigma \le 1; \end{cases} \tag{3.13}$$

see Figure 3. Note that we use the notation $G = G(\sigma; P)$ to denote the dependence on the numerical Peclet number P. For constant s we can evalute the integral in (3.11) and recover the constant coefficient flux (3.6b).

The Green's function (3.13) for the flux has the following properties. First, it is discontinuous at $\sigma = \frac{1}{2}$, corresponding to $x = x_\mathrm{e}$, with jump $G(\frac{1}{2}-; P) - G(\frac{1}{2}+; P) = 1$. Second, the function has a clear bias towards the upwind side of the interval when $|P| \gg 1$, which means that for dominant advection the upwind value of the source term is the relevant one. On the other hand, for dominant diffusion, i.e., $|P|$ is small, the average value $\frac{1}{2} - W(P)$ is close to 0, implying that the inhomogeneous flux is not important. Finally, it satisfies the symmetry property $G(\sigma; P) = -G(1 - \sigma; -P)$.

When only $m(x) = \mathrm{Const} \neq 0$ on $[x_\mathrm{C}, x_\mathrm{E}]$, the expression for the inhomogeneous flux can be written as

$$f_\mathrm{e}^{(\mathrm{i})} = \Delta x \int_0^1 G\big(\sigma; \langle \lambda, 1 \rangle\big) s(x(\sigma))\, \mathrm{d}\sigma, \tag{3.14}$$

with $G(\sigma; P)$ defined in (3.13) and where σ is a *weighted* normalised coordinate defined by

$$\sigma(x) := \int_{x_\mathrm{C}}^{x} \lambda(\xi)\,\mathrm{d}\xi / \langle \lambda, 1\rangle. \tag{3.15}$$

Note that $\sigma'(x) > 0$ implying that $\sigma(x)$ is monotonically increasing from 0 to 1 indeed.

To summarize, the flux f_e is the superposition (3.5a) of the homogeneous flux $f_\mathrm{e}^{(\mathrm{h})}$ given in (3.10a) and the inhomogeneous flux $f_\mathrm{e}^{(\mathrm{i})}$ given in (3.11). Our numerical approximation of the homogeneous flux will be based on (3.10a). To approximate the inhomogeneous flux, we will not use (3.11), however, instead we assume $m(x) = \mathrm{Const}$ on $[x_\mathrm{C}, x_\mathrm{E}]$ and employ the representation (3.14), with $G(\sigma; P)$ the constant coefficient Green's function given in (3.13).

4 Derivation of the numerical flux

In this section we give quadrature rules for the inner products $\langle \lambda, 1\rangle$ and $\langle a, \mathrm{e}^{-\Lambda}\rangle$, $(a = \lambda, \varepsilon^{-1})$. This readily gives an approximation of (3.10a). Moreover, we propose an approximation for the integral in (3.14). Our objective is to obtain a numerical flux approximation that is second order accurate, uniformly in the local Peclet numbers.

First, we introduce the average $\bar{a}_\mathrm{e}$, the weighted average $\tilde{a}_\mathrm{e}$ and the upwind value $a_\mathrm{u,e}$ of a variable $a = a(x)$ defined on $[x_\mathrm{C}, x_\mathrm{E}]$ as follows

$$\bar{a}_\mathrm{e} := \tfrac{1}{2}(a_\mathrm{C} + a_\mathrm{E}), \tag{4.1a}$$

$$\tilde{a}_\mathrm{e} := W(-\bar{P}_\mathrm{e})a_\mathrm{C} + W(\bar{P}_\mathrm{e})a_\mathrm{E}, \tag{4.1b}$$

$$a_\mathrm{u,e} := \begin{cases} a_\mathrm{C} & \text{if} \quad \bar{P}_\mathrm{e} \geq 0, \\ a_\mathrm{E} & \text{if} \quad \bar{P}_\mathrm{e} < 0. \end{cases} \tag{4.1c}$$

The weights in the expression for $\tilde{a}_\mathrm{e}$ are determined by the average Peclet number $\bar{P}_\mathrm{e}$. Note that the weighted average $\tilde{a}_\mathrm{e}$ reduces to the ordinary average $\bar{a}_\mathrm{e}$ for $\bar{P}_\mathrm{e} \to 0$ and to $a_\mathrm{u,e}$ for $|\bar{P}_\mathrm{e}| \to \infty$. This is also apparent from the following relation

$$\tilde{a}_\mathrm{e} = 2W(|\bar{P}_\mathrm{e}|)\bar{a}_\mathrm{e} + \big(1 - 2W(|\bar{P}_\mathrm{e}|)\big)a_\mathrm{u,e}, \tag{4.2}$$

which can be readily verified from (4.1). In the derivation of the numerical flux that follows, we need the 'product rule'

$$\tilde{a}_\mathrm{e}\tilde{b}_\mathrm{e} = \widetilde{(ab)}_\mathrm{e} - W(\bar{P}_\mathrm{e})W(-\bar{P}_\mathrm{e})(a_\mathrm{E} - a_\mathrm{C})(b_\mathrm{E} - b_\mathrm{C}). \tag{4.3}$$

A similar rule for $\bar{a}_\mathrm{e}$ can be easily derived substituting $\bar{P}_\mathrm{e} = 0$ in (4.3).

For the inner product $\langle \lambda, 1\rangle$ we use the standard trapezoidal rule, which can be written as

$$\langle \lambda, 1\rangle = \bar{P}_\mathrm{e} - \tfrac{1}{12}\lambda''(\xi)\Delta x^3, \quad \xi \in (x_\mathrm{C}, x_\mathrm{E}). \tag{4.4}$$

In the derivation of the trapezoidal rule (4.4) we have replaced λ by its linear interpolant on $[x_\mathrm{C}, x_\mathrm{E}]$, however, this is not a suitable approach for the inner products $\langle a, \mathrm{e}^{-\Lambda}\rangle$. Instead, we approximate both a and Λ by their linear interpolants, resulting in the following generalized trapezoidal rule

$$\frac{\langle a, \mathrm{e}^{-\Lambda}\rangle}{\langle 1, \mathrm{e}^{-\Lambda}\rangle} = \tilde{a}_\mathrm{e} + E_\mathrm{e}(a), \quad |E_\mathrm{e}(a)| < C\Delta x^2, \tag{4.5}$$

for some $C > 0$, which holds provided a is twice and P once continuously differentiable on $(x_{\rm C}, x_{\rm E})$. For a proof of this rule see [6].

For the homogeneous flux (3.10a) we need to evalute the first argument of $\mathcal{F}^{\rm h}$. Applying the quadrature rules (4.4), (4.5) and the product rule (4.3), with $a = \varepsilon$ and $b = \varepsilon^{-1}$, we can derive the following approximation

$$\frac{\langle \lambda, {\rm e}^{-\Lambda}\rangle / \langle \lambda, 1\rangle}{\langle \varepsilon^{-1}, {\rm e}^{-\Lambda}\rangle} \doteq \frac{1}{\bar{P}_{\rm e}} \frac{\tilde{\lambda}_{\rm e}}{\widetilde{\left(\varepsilon^{-1}\right)}_{\rm e}} \doteq \frac{1}{\bar{P}_{\rm e}} \tilde{\varepsilon}_{\rm e} \tilde{\lambda}_{\rm e} = \frac{\tilde{P}_{\rm e}}{\bar{P}_{\rm e}} \frac{\tilde{\varepsilon}_{\rm e}}{\Delta x}. \tag{4.6}$$

Substituting this expression in (3.10a) we obtain the homogeneous numerical flux

$$F_{\rm e}^{\rm (h)} = \mathcal{F}^{\rm h}\Big(\frac{\tilde{P}_{\rm e}}{\bar{P}_{\rm e}} \frac{\tilde{\varepsilon}_{\rm e}}{\Delta x}, \bar{P}_{\rm e}; \varphi_{\rm C}, \varphi_{\rm E}\Big), \tag{4.7}$$

which is in fact the constant coefficient flux defined in (3.6a) and (3.8), with ε and P replaced by$\tilde{P}_{\rm e}\tilde{\varepsilon}_{\rm e}/\bar{P}_{\rm e}$ and $\bar{P}_{\rm e}$, respectively.

For the inhomogeneous flux we note that the Green's function $G(\sigma; P)$ has a clear bias towards the upwind side of the interval when $|P| \gg 1$. For that reason we replace $s(x(\sigma))$ in (3.14) by its upwind value and evaluate the resulting integral exactly. This way we obtain for the inhomogeneous numerical flux

$$F_{\rm e}^{\rm (i)} = \big(\tfrac{1}{2} - W(\bar{P}_{\rm e})\big) s_{\rm u,e}\, \Delta x, \tag{4.8}$$

which is the constant coefficient flux (3.6b) with P and s replaced by $\bar{P}_{\rm e}$ and $s_{\rm u,e}$, respectively.

The final numerical flux $F_{\rm e}$ is the superposition of the homogeneous part $F_{\rm e}^{\rm (h)}$ and the inhomogeneous part $F_{\rm e}^{\rm (i)}$, i.e.,

$$F_{\rm e} = F_{\rm e}^{\rm (h)} + F_{\rm e}^{\rm (i)}, \tag{4.9}$$

with $F_{\rm e}^{\rm (h)}$ and $F_{\rm e}^{\rm (i)}$ given in (4.7) and (4.8), respectively; see also [6]. We refer to the flux approximation in (4.7)-(4.9) as the *complete flux* (CF) scheme. This scheme has to be combined with the discrete conservation law (2.5) to obtain the final scheme. This is detailed in the next section.

5 The finite volume-complete flux scheme

In this section we adopt the index notation as in Section 2. The numerical flux at the eastern cell interface $x_{j+1/2}$ of the control volume I_j can be written as in (2.6), i.e.,

$$F_{j+1/2} = \alpha_{j+1/2}\, \varphi_j - \beta_{j+1/2}\, \varphi_{j+1} + \gamma_{j+1/2}\, s_j + \delta_{j+1/2}\, s_{j+1}, \tag{5.1a}$$

where the coefficients $\alpha_{j+1/2}$, $\beta_{j+1/2}$ etc. are defined by

$$\begin{aligned}
&\alpha_{j+1/2} := \frac{\mathcal{E}_{j+1/2}}{\Delta x} B^-_{j+1/2}, \quad \beta_{j+1/2} := \frac{\mathcal{E}_{j+1/2}}{\Delta x} B^+_{j+1/2},\\
&\gamma_{j+1/2} = \max\big(\tfrac{1}{2} - W^+_{j+1/2}, 0\big)\, \Delta x, \quad \delta_{j+1/2} = \min\big(\tfrac{1}{2} - W^+_{j+1/2}, 0\big)\, \Delta x,\\
&\mathcal{E}_{j+1/2} := \frac{\tilde{P}_{j+1/2}}{\bar{P}_{j+1/2}}\, \tilde{\varepsilon}_{j+1/2}, \quad B^\pm_{j+1/2} := B\big(\pm \bar{P}_{j+1/2}\big), \quad W^+_{j+1/2} := W\big(\bar{P}_{j+1/2}\big).
\end{aligned} \tag{5.1b}$$

(Weighted) average/upwind values like $\tilde{P}_{j+1/2}$ are defined analogous to (4.1). A similar expression holds for the numerical flux $F_{j-1/2}$ at the western cell interface $x_{j-1/2}$. Substituting these in the discrete conservation law (2.5) we obtain

$$-a_{\mathrm{W},j}\varphi_{j-1} + a_{\mathrm{C},j}\varphi_j - a_{\mathrm{E},j}\varphi_{j+1} = b_{\mathrm{W},j}s_{j-1} + b_{\mathrm{C},j}s_j + b_{\mathrm{E},j}s_{j+1}, \tag{5.2}$$

referred to as the *finite volume-complete flux* (FV-CF) scheme, with the coefficients $a_{\mathrm{W},j}$, $b_{\mathrm{W},j}$ etc. defined by

$$\begin{aligned} &a_{\mathrm{W},j} := \alpha_{j-1/2}, \quad a_{E,j} := \beta_{j+1/2}, \qquad a_{C,j} := \alpha_{j+1/2} + \beta_{j-1/2}, \\ &b_{\mathrm{W},j} := \gamma_{j-1/2}, \quad b_{\mathrm{E},j} := -\delta_{j+1/2} \quad b_{\mathrm{C},j} = \Delta x - \gamma_{j+1/2} + \delta_{j-1/2}. \end{aligned} \tag{5.3}$$

Note that $b_{\mathrm{W},j}, b_{\mathrm{E},j}, b_{\mathrm{C},j} \geq 0$ and $b_{\mathrm{W},j} + b_{\mathrm{C},j} + b_{\mathrm{E},j} = \Delta x\big(1 + W^+_{j+1/2} - W^+_{j-1/2}\big)$. The FV-CF scheme has a three-point coupling for both φ and s, resulting in the following linear system

$$\boldsymbol{A\varphi} = \boldsymbol{Bs} + \boldsymbol{b}, \tag{5.4}$$

where $\boldsymbol{\varphi}$ and $\boldsymbol{s}$ are the vector of unknowns and source terms, respectively, and where the vector $\boldsymbol{b}$ contains the boundary data. Both matrices $\boldsymbol{A}$ and $\boldsymbol{B}$ are tridiagonal. For the special case of constant m and ε, we can easily prove that $a_{\mathrm{W},j}, a_{\mathrm{E},j} \geq 0$ and $a_{\mathrm{C},j} = a_{\mathrm{W},j} + a_{\mathrm{E},j}$, and as a consequence the matrix $\boldsymbol{A}$ is an M-matrix, provided not both boundary conditions are of Neumann type.

In our numerical examples in Section 6 we compare the CF scheme for the flux approximation with the *homogeneous flux* (HF) scheme. The HF scheme is the numerical scheme that follows if we approximate the flux by the homogeneous flux only. This means that $\gamma_{j+1/2} = \delta_{j+1/2} = 0$ in (5.1a) and hence $b_{\mathrm{W},j} = b_{\mathrm{E},j} = 0$ and $b_{\mathrm{C},j} = \Delta x$ in (5.2).

It is instructive to consider some limiting cases of the FV-CF scheme. First, we take $m = 0$, i.e., we consider the equation $-\big(\varepsilon\varphi'\big)' = s$. In this case $\bar{P}_{j\pm1/2} = 0$ and consequently the inhomogeneous fluxes vanish, resulting in the second order central difference scheme

$$-\frac{1}{\Delta x}\Big(\bar{\varepsilon}_{j+1/2}\big(\varphi_{j+1} - \varphi_j\big) - \bar{\varepsilon}_{j-1/2}\big(\varphi_j - \varphi_{j-1}\big)\Big) = s_j\,\Delta x. \tag{5.5}$$

Another limiting case is $\varepsilon = 0$, corresponding to the reduced equation $\big(m\varphi\big)' = s$. For this equation we have to distinguish between $m > 0$ and $m < 0$. In the former case, $\bar{P}_{j\pm1/2} \to +\infty$ and the FV-CF scheme reduces to

$$m_j\varphi_j - m_{j-1}\varphi_{j-1} = \tfrac{1}{2}\big(s_{j-1} + s_j\big)\,\Delta x. \tag{5.6a}$$

In the latter case, $\bar{P}_{j\pm1/2} \to -\infty$, giving the scheme

$$m_{j+1}\varphi_{j+1} - m_j\varphi_j = \tfrac{1}{2}\big(s_j + s_{j+1}\big)\,\Delta x. \tag{5.6b}$$

Both schemes (5.6) are second order approximations for the reduced equation. Here we see why it is important that our flux representation is based on the entire equation. Standard methods like the HF scheme omit the inhomogeneous flux, so that the schemes in (5.6) further reduce to $m_j\varphi_j - m_{j-1}\varphi_{j-1} = s_j\Delta x$ for $m > 0$ and $m_{j+1}\varphi_{j+1} - m_j\varphi_j = s_j\Delta x$ for $m < 0$, which is just the first order upwind scheme for the reduced advection-reaction equation.

From these observations we conclude that the FV-CF scheme (5.2) can be interpreted as a combination of the central difference scheme (5.5) and the schemes (5.6), the combination determined by the (average) Peclet numbers $\bar{P}_{j\pm1/2}$.

6 Numerical examples

In this section we apply the CF and HF schemes to two model problems to assess their (order of) accuracy. We consider both diffusion-dominated and advection-dominated flow. Moreover, we demonstrate the feasibility of the CF scheme to compute a shock layer solution of the compressible Navier-Stokes equations.

Example 1. Advection-diffusion-reaction equation with boundary layer at outflow.
We solve the BVP [23]

$$\big(m\varphi - \varepsilon\varphi'\big)' = s, \quad 0 < x < 1, \tag{6.1a}$$

$$\varphi(0) = 0, \quad \varphi(1) = 1, \tag{6.1b}$$

with mass flux $m(x) = 1 - b\sin\pi x$ and source term s chosen such that the exact solution is given by

$$\varphi(x) = a\sin(\pi x) + \frac{\mathrm{e}^{(x-1)/\varepsilon} - \mathrm{e}^{-1/\varepsilon}}{1 - \mathrm{e}^{-1/\varepsilon}}. \tag{6.2}$$

Note that for $0 < \varepsilon \ll 1$ the solution has a thin boundary layer of width ε near $x = 1$. We take the following parameter values: $a = 0.2$, $b = -0.95$ and $\varepsilon = 1$ (dominant diffusion) or $\varepsilon = 10^{-5}$ (dominant advection). Let $h = \Delta x = 1/(N-1)$ be the grid size, with N the number of grid points. To determine the accuracy of a numerical solution we compute the average error $e^h := ||\boldsymbol{\varphi} - \boldsymbol{\varphi}^*||_1/N$, where $\boldsymbol{\varphi}^*$ denotes the exact solution restricted to the grid, as a function of the reciprocal grid size h^{-1}. Table 1 shows e^h and the reduction factors $e^h/e^{h/2}$ for $\varepsilon = 1$. Clearly, $e^h/e^{h/2} \to 4$ for $h \to 0$ for both the HF and CF scheme, and consequently, both schemes display second order convergence behaviour for $h \to 0$. The numerical errors are approximately the same for both schemes. However, the situation is quite different for the case $\varepsilon = 10^{-5}$ shown in Table 2. In this case $e^h/e^{h/2} \to 2$ for $h \to 0$ for the HF scheme, which means that the method is only first order convergent, in agreement with the observation that the HF-scheme reduces to the first order upwind scheme for the advection-reaction equation; see Section 5. The CF-scheme still displays second order convergence behaviour, which is consistent with the reduction of the CF-scheme to the scheme (5.6) for the advection-reaction equation. Obviously, the CF-solution is in this case much more accurate than the HF-solution.

	CF		HF	
h^{-1}	e^h	$e^h/e^{h/2}$	e^h	$e^h/e^{h/2}$
10	2.201×10^{-3}	3.69	1.823×10^{-3}	3.81
20	5.967×10^{-4}	3.84	4.779×10^{-4}	3.90
40	1.553×10^{-4}	3.92	1.224×10^{-4}	3.95
80	3.963×10^{-5}	3.96	3.098×10^{-5}	3.97
160	1.001×10^{-5}	3.98	7.794×10^{-6}	3.99
320	2.515×10^{-6}	3.99	1.955×10^{-6}	3.99
640	6.303×10^{-7}	3.99	4.894×10^{-7}	4.00
1280	1.578×10^{-7}		1.224×10^{-7}	

Table 1: Example 1, errors for diffusion-dominated flow. Parameter values are: $a = 0.2$, $b = -0.95$ and $\varepsilon = 1$.

	CF		HF	
h^{-1}	e^h	$e^h/e^{h/2}$	e^h	$e^h/e^{h/2}$
10	2.146×10^{-3}	3.82	1.977×10^{-2}	1.86
20	5.613×10^{-4}	3.91	1.061×10^{-2}	1.93
40	1.436×10^{-4}	3.95	5.504×10^{-3}	1.97
80	3.632×10^{-5}	3.98	2.801×10^{-3}	1.99
160	9.121×10^{-6}	4.00	1.411×10^{-3}	2.00
320	2.280×10^{-6}	4.02	7.070×10^{-4}	2.01
640	5.669×10^{-7}	4.05	3.525×10^{-4}	2.02
1280	1.399×10^{-7}		1.746×10^{-4}	

Table 2: Example 1, errors for advection-dominated flow. Parameter values are: $a = 0.2$, $b = -0.95$ and $\varepsilon = 10^{-5}$.

Example 2. Advection-diffusion-reaction equation with interior layer.
We solve the BVP [11]

$$\big(m\varphi - \varepsilon\varphi'\big)' = s, \quad 0 < x < 1, \tag{6.3a}$$
$$\varphi(0) = \varphi'(1) = 0, \tag{6.3b}$$

where the mass flux m and the source term s are given by

$$m(x) = (1+x)^3, \quad s(x) = \frac{s_{\max}}{1 + s_{\max}(2x-1)^2}, \tag{6.4}$$

respectively. The mass flux is a smoothly varying function of x whereas the source term has a sharp peak at $x = \frac{1}{2}$, causing a steep interior layer, provided $0 < \varepsilon \ll 1$; see Figure 4.

For this BVP there is no exact solution available. In order to assess the order of accuracy of both schemes, we compute numerical approximations of $\varphi(\frac{1}{2})$ with increasingly smaller grid sizes and apply Richardson extrapolation to these results; see e.g. [15]. More precisely, let

$$\varphi(\tfrac{1}{2}) = \varphi^h + e^h = \varphi^{h/2} + e^{h/2} = \varphi^{h/4} + e^{h/4}, \quad h = \Delta x, \tag{6.5}$$

where φ^h denotes the numerical approximation of $\varphi(\frac{1}{2})$ computed with grid size h and e^h the corresponding (global) discretisation error, etc. Assuming the following error expansion

$$e^h = Ch^p + \mathcal{O}\big(h^q\big), \quad q > p, \tag{6.6}$$

we can derive the following relation for the order of accuracy p:

$$2^p \doteq \frac{\varphi^{h/2} - \varphi^h}{\varphi^{h/4} - \varphi^{h/2}} =: r^h. \tag{6.7}$$

The r^h-values are presented in Table 3. From this table it is evident that for dominant diffusion, i.e., $\varepsilon = 10^{-1}$, both HF and CF scheme are second order convergent for $h \to 0$. On the other hand, for dominant advection, i.e., $\varepsilon = 10^{-8}$, the HF scheme shows first order convergence for $h \to 0$, whereas the CF scheme is still second order convergent. The large entries for $h^{-1} = 10, 20$ in the last column of the table indicate that the approximation (6.7) is not yet valid, or equivalently, the higher order terms in

	$\varepsilon = 10^{-1}$		$\varepsilon = 10^{-8}$	
h^{-1}	HF	CF	HF	CF
10	4.41	6.76	2.39	2.36×10^1
20	4.54	6.00	1.97	-2.92×10^2
40	4.08	3.65	1.96	2.57
80	4.02	3.62	1.98	4.00
160	4.00	3.77	1.99	4.00
320	4.00	3.88	1.99	4.00
640	4.00	3.94	2.00	4.00
1280	4.00	3.97	2.00	4.00

Table 3: Example 2, the r^h-values for the complete flux scheme and the homogeneous flux scheme as a function of h^{-1}, for maximum source term $s_{\max} = 10^2$.

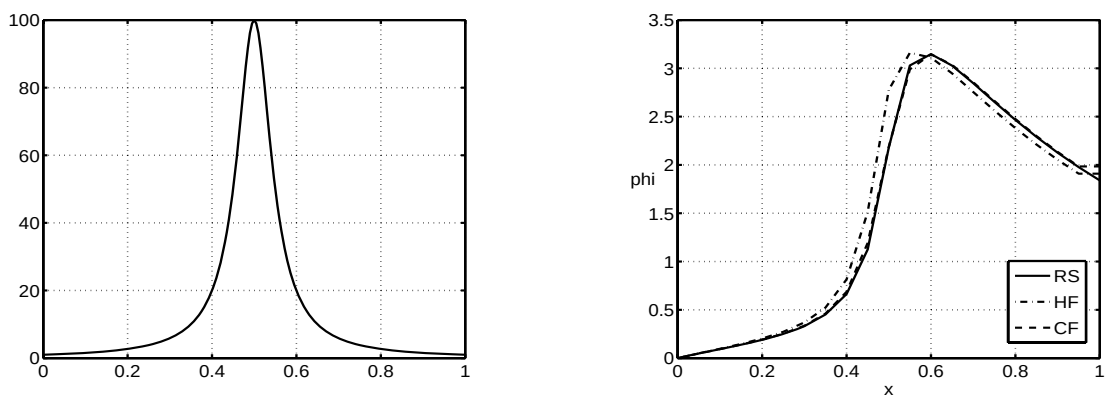

Figure 4: Example 2, the source term s (left) and the corresponding (numerical) solution (right) of (6.3). Parameter values are $\varepsilon = 10^{-8}$, $s_{\max} = 10^2$ and $h^{-1} = 20$.

(6.6) can not be neglected, and more importantly, that the CF-solution is already rather acurate even on these coarse grids. This is confirmed in Figure 4 which shows the HF and CF solutions compared to the reduced solution (RS) of the problem $(m\varphi)' = s,\ \varphi(0) = 0$.

Example 3. Shock layer solution for the compressible Navier-Stokes equations [12].
We apply the FV-CF scheme to the (dimensionless) compressible Navier-Stokes equations on the interval $(0, 1)$, i.e.,

$$\big(u - \varepsilon u'\big)' = \frac{-1}{\gamma \mathrm{Ma}^2} p', \tag{6.8a}$$

$$\big(T - \alpha T'\big)' = (1-\gamma) p u' + \varepsilon \gamma (\gamma - 1) \mathrm{Ma}^2 \big(u'\big)^2, \tag{6.8b}$$

$$T = pu, \tag{6.8c}$$

$$u(0) = T(0) = p(0) = 1, \quad u'(1) = T'(1) = p'(1) = 0, \tag{6.8d}$$

where $u > 0$ is the velocity, T the temperature and p the pressure, all scaled with their value at the inlet

$x = 0$. Parameters in (6.8) are $\varepsilon := 4/(3\mathrm{Re})$, with Re the Reynolds number, $\alpha := \gamma/(\mathrm{Pe})$, with Pe the Peclet number and γ the specific heat ratio, and Ma the Mach number (at the inlet). The BVP (6.8) is a model problem for one-dimensional steady compressible flow. Equation (6.8a) describes conservation of momentum, equation (6.8b) conservation of energy and (6.8c) is the equation of state for a perfect gas. Note that the continuity equation is missing since the (scaled) mass flux $m(x) = 1$. For supersonic inflow, i.e., $\mathrm{Ma} > 1$, system (6.8) has a shock layer connecting the constant states at inflow and outflow.

Both conservation laws (6.8a) and (6.8b) can be written in the standard form (2.1) with source terms s_u and s_T, respectively, given by

$$s_u := \frac{-1}{\gamma \mathrm{Ma}^2} p', \quad s_T := (1-\gamma) p u' + \varepsilon \gamma (\gamma - 1) \mathrm{Ma}^2 \big(u'\big)^2. \tag{6.9}$$

The source term s_u is proportional to the pressure gradient, which drives the flow. The first term in s_T describes compression of the gas and the second viscous dissipation. When applying the FV-CF scheme to (6.8), we need to address a few issues that are not standard. First, we can integrate equation (6.8a) *exactly* over a control volume I_j, to find

$$f_u\big(x_{j+1/2}\big) - f_u\big(x_{j-1/2}\big) + \frac{1}{\gamma \mathrm{Ma}^2}\big(p\big(x_{j+1/2}\big) - p\big(x_{j-1/2}\big)\big) = 0, \tag{6.10}$$

where $f_u := u - \varepsilon u'$ is the flux corresponding to equation (6.8a). Second, we can evaluate the integral of s_u exactly, compare (3.2), and can derive from (3.10b) the following expression for the inhomogeneous flux

$$f^{(\mathrm{i})}_{u,j+1/2} = \frac{1}{\gamma \mathrm{Ma}^2}\big(\tilde{p}_{j+1/2} - p\big(x_{j+1/2}\big)\big). \tag{6.11}$$

Substituting (6.11) in (6.10) we obtain the following discrete conservation law

$$F^{(\mathrm{h})}_{u,j+1/2} - F^{(\mathrm{h})}_{u,j-1/2} + \frac{1}{\gamma \mathrm{Ma}^2}\big(\tilde{p}_{j+1/2} - \tilde{p}_{j-1/2}\big) = 0, \tag{6.12}$$

where $F^{(\mathrm{h})}_{u,j+1/2}$ is the homogeneous numerical flux for equation (6.8a). This equation replaces the discrete conservation law corresponding to (2.5) and we only need to compute the homogeneous flux from (4.7). Finally, the source term s_T contains the derivative u'. In order to approximate $u'(x_j)$ we compute u on the adjacent intervals $[x_{j-1}, x_j]$ and $[x_j, x_{j+1}]$ from the homogeneous momentum equation $\big(u - \varepsilon u'\big)' = 0$, compute its values at $x_{j\pm 1/2}$ and apply the standard central difference approximation as follows:

$$\begin{aligned} u'(x_j) &\doteq \frac{1}{\Delta x}\big(u\big(x_{j+1/2}\big) - u\big(x_{j-1/2}\big)\big) \\ &= \frac{1}{\Delta x}\big(A(-P_u/2)(u_j - u_{j-1}) + A(P_u/2)(u_{j+1} - u_j)\big), \end{aligned} \tag{6.13}$$

where $P_u := \varepsilon/\Delta x$ is the (numerical) Peclet number for the momentum equation (6.8a) and where the function $A(z)$ is defined by

$$A(z) := \frac{1}{\mathrm{e}^z + 1}. \tag{6.14}$$

It is easy to verify that A satisfies $0 \le A(z) \le 1$ and $A(-z) + A(z) = 1$, so that we can interpret the difference approximation in (6.13) as a weighted average of the forward and backward difference approximations.

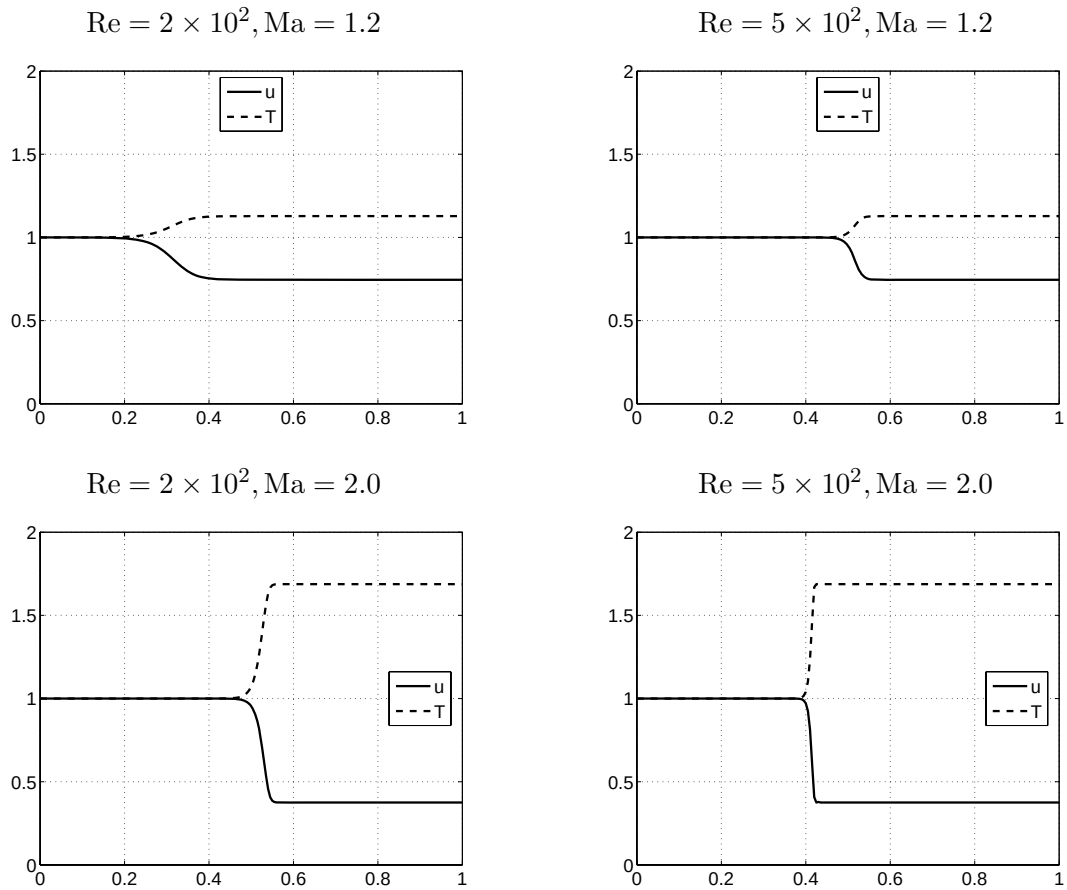

Figure 5: Solutions of boundary value problem (6.8) for $\mathrm{Re} = 2 \times 10^2, 5 \times 10^2$ and $\mathrm{Ma} = 1.2, 2.0$. Other parameter values are $\mathrm{Pr} = \mathrm{Pe}/\mathrm{Re} = 0.72$, $\gamma = 1.4$ and $\Delta x = 5 \times 10^{-3}$.

The final FV-CF scheme gives a nonlinear, (block) tridiagonal system for the unknowns $\boldsymbol{u} = (u_j)$ and $\boldsymbol{T} = (T_j)$, which we solve using Newton iteration in combination with continuation in Re; see e.g. [2]. The first initial guess is computed from a scalar ODE valid for $\mathrm{Pe}/\mathrm{Re} = 0.75$. As an example, we present four solutions in Figure 5. Clearly, the jump across the shock layer increases with increasing Ma whereas its width decreases with increasing Re and/or increasing Ma, confirming the analysis in [12].

7 Summary and conclusions

We have derived an integral representation for the flux of the advection-diffusion-reaction equation from a local BVP for the *entire* equation, including the source term. As a consequence, the flux consists of two parts, i.e., a homogeneous and an inhomogeneous part, corresponding to the homogeneous and particular solution of the BVP, respectively. A new representation of the inhomogeneous flux in terms of a Green's function is given. Combining this integral representation with suitable quadrature rules, we could derive expressions for the numerical flux. Obviously, also the numerical flux consists of a homogeneous and an inhomogeneous part. The inhomogeneous numerical flux turns out to be very important for dominant

advection, since it ensures that the flux approximation remains second order accurate. Combining the complete flux scheme with a standard finite volume discretisation, we obtain the finite volume-complete flux scheme. This scheme turns out to be second order accurate, uniformly in the local Peclet numbers, does not generate spurious oscillations, and moreover, has only a three-point coupling.

This paper is meant to be the framework for further research on this topic. Currently, we are extending our research in the following directions. First, we combine the integral representation of the flux with more accurate quadrature rules to derive higher order schemes. Second, we work on a complete flux scheme for two-dimensional problems, and finally, we will extend the complete flux scheme to time-dependent problems. Preliminary results are very promising and will be reported elsewhere. Finally, a version of the complete flux scheme for spherically symmetric conservation laws is already presented in [21].

References

[1] D. Allen and R. Southwell, Relaxation methods applied to determining the motion, in two dimensions, of a viscous fluid past a fixed cylinder, *Quart. J. Mech. Appl. Math.* 8, 129-145, 1955.

[2] U.M. Ascher, R.M.M. Mattheij and R.D. Russell, *Numerical Solution of Boundary Value Problems for Ordinary Differential Equations*, Prentice Hall Series in Computational Mathematics, Prentice Hall, Englewood Cliffs,1988.

[3] R.E. Bank, D.J. Rose and W. Fichtner, Numerical methods for semiconductor device simulation, *IEEE Trans. El. Dev.* 30, 1031-1041, 1983.

[4] T.M. El-Mistikawy and M.J. Werle, Numerical methods for boundary layers with blowing- the exponential box scheme, *AIAA J.* 16, 749-751, 1978.

[5] R. Eymard, T. Gallouët and R. Herbin, Finite volume methods, in: P.G. Ciarlet and J.L. Lions (eds.), *Handbook of Numerical Analysis, Volume VII*, North-Holland, Amsterdam, 2000, pp. 713-1020.

[6] B. van 't Hof, J.H.M. ten Thije Boonkkamp and R.M.M. Mattheij, Discretisation of the stationary convection-diffusion-reaction equation, *Numer. Meth. for Part. Diff. Eq.* 14, 607-625, 1998.

[7] A.M. Il'in, Differencing scheme for a differential equation with a small parameter affecting the highest derivative, *Mat. Zametki* 6, 237-248, 1969 (in Russian).

[8] J.W. Jerome, *Analysis of Charge transport*, Springer, Berlin, 1996.

[9] Randell J. LeVeque, *Finite Volume Methods for Hyperbolic Problems*, Cambridge Texts in Applied Mathematics, Cambridge University Press, Cambridge, 2002.

[10] P.A. Markowich, C.A. Ringerhofer and C. Schmeiser, *Semiconductor Equations*, Springer, Vienna, 1990.

[11] K.W. Morton, *Numerical Solution of Convection-Diffusion Problems*, Applied Mathematics and Mathematical Computation 12, Chapman & Hall, London, 1996.

[12] Shih-I Pai, *Viscous Flow Theory, I-Laminar Flow*, Van Nostrand Company, Inc., Princeton, 1956.

[13] S.V. Patankar, *Numerical Heat Transfer and Fluid Flow*, Series in Computational Methods in Mechanics and Thermal Sciences, Hemishere Publishing Corporation, New York, 1980.

[14] T. Poinsot and D. Veynante, *Theoretical and Numerical Combustion, Second Edition*, Edwards, Philadelphia, 2005.

[15] A. Quarteroni, R. Sacco and F. Saleri, *Numerical Mathematics*, Texts in Applied Mathematics 37, Springer, New York, 2000.

[16] W.H.A. Schilders, Application of exponential fitting techniques to semiconductor device simulation. In: J.J.H. Miller (ed.), *Computational Methods for Boundary and Interior Layers*, Boole Press, Dublin, 1991, pp. 175-202.

[17] Chi-Wang Shu, Essentially non-oscillatory and weighted essentially non-oscillatory schemes for hyperbolic conservation laws, in: A. Quarteroni (ed.), *Advanced Numerical Approximation of Nonlinear Hyperbolic Equations*, Lecture Notes in Mathematics 1697, Springer, Berlin, 1998, pp. 325-432.

[18] D.B. Spalding, A novel finite difference formulation for differential expressions involving both first and second derivatives. *Int. J. Num. Meth. in Eng.* 4, 551-559, 1972.

[19] G.D. Thiart, Finite difference scheme for the numerical solution of fluid flow and heat transfer problems on nonstaggered grids, *Numer. Heat Transfer, Part B* 17, 41-62, 1990.

[20] G.D. Thiart, Improved finite-difference scheme for the solution of convection-diffusion problems with the SIMPLEN algorithm, *Numer. Heat Transfer, Part B* 18, 81-95, 1990.

[21] J.H.M. ten Thije Boonkkamp and M.J.H. Anthonissen, The complete flux scheme for spherically symmetric conservation laws, In: M. Bubak et al. (eds.): *ICCS 2008, Part I, LNCS 5101*, Springer, Berlin, 2008, pp. 651-660.

[22] J.H.M. ten Thije Boonkkamp and W.H.A. Schilders, An exponential fitting scheme for the electrothermal device equations specifically for the simulation of avalanche generation, *COMPEL* 12, 95-11, 1993.

[23] P. Wesseling, *Principles of Computational Fluid Dynamics*, Springer Series in Computational Mathematics 29, Springer, Berlin, 2000.

[24] Forman A. Williams, *Combustion Theory, Second Edition*, Addison-Wesley, Redwood City, 1985.